2-15-2003

Trace Gas and Particle Emissions from Fires in Large Diameter and Belowground Biomass Fuels

Isaac T. Bertschi
University of Montana - Missoula

Robert J. Yokelson
University of Montana - Missoula, bob.yokelson@umontana.edu

Darold E. Ward
USDA Forest Service - Rocky Mountain Research Station

R. E. Babbitt
USDA Forest Service - Fire Sciences Laboratory

Ronald A. Susott
USDA Forest Service - Rocky Mountain Research Station

See next page for additional authors

Recommended Citation

Bertschi, I., R. J. Yokelson, D. E. Ward, R. E. Babbitt, R. A. Susott, J. G. Goode, and W. M. Hao, Trace gas and particle emissions from fires in large diameter and belowground biomass fuels, J. Geophys. Res., 108(D13), 8472, doi:10.1029/2002JD002100, 2003.

Trace gas and particle emissions from fires in large diameter and belowground biomass fuels

Isaac Bertschi,[1,2] Robert J. Yokelson,[1] Darold E. Ward,[3,4] Ron E. Babbitt,[3] Ronald A. Susott,[3] Jon G. Goode,[1,5] and Wei Min Hao[3]

Received 15 January 2002; revised 30 July 2002; accepted 6 August 2002; published 15 February 2003.

[1] We adopt a working definition of residual smoldering combustion (RSC) as biomass combustion that produces emissions that are not lofted by strong fire-induced convection. RSC emissions can be produced for up to several weeks after the passage of a flame front and they are mostly unaffected by flames. Fuels prone to RSC include downed logs, duff, and organic soils. Limited observations in the tropics and the boreal forest suggest that RSC is a globally significant source of emissions to the troposphere. This source was previously uncharacterized. We measured the first emission factors (EF) for RSC in a series of laboratory fires and in a wooded savanna in Zambia, Africa. We report EF_{RSC} for both particles with diameter <2.5 μm (PM2.5) and the major trace gases as measured by open-path Fourier transform infrared (OP-FTIR) spectroscopy. The major trace gases include carbon dioxide, carbon monoxide, methane, ethane, ethene, acetylene, propene, formaldehyde, methanol, acetic acid, formic acid, glycolaldehyde, phenol, furan, ammonia, and hydrogen cyanide. We show that a model used to predict trace gas EF for fires in a wide variety of aboveground fine fuels fails to predict EF for RSC. For many compounds, our EF for RSC-prone fuels from the boreal forest and wooded savanna are very different from the EF for the same compounds measured in fire convection columns above these ecosystems. We couple our newly measured EF_{RSC} with estimates of fuel consumption by RSC to refine emission estimates for fires in the boreal forest and wooded savanna. We find some large changes in estimates of biomass fire emissions with the inclusion of RSC. For instance, the wooded savanna methane EF increases by a factor of 2.5 even when RSC accounts for only 10% of fuel consumption. This shows that many more measurements of fuel consumption and EF for RSC are needed to improve estimates of biomass burning emissions. *INDEX TERMS:* 0345 Atmospheric Composition and Structure: Pollution—urban and regional (0305); 0368 Atmospheric Composition and Structure: Troposphere—constituent transport and chemistry; 0394 Atmospheric Composition and Structure: Instruments and techniques; 0365 Atmospheric Composition and Structure: Troposphere—composition and chemistry; *KEYWORDS:* biomass burning, smoldering combustion, oxygenated organic compounds, ammonia, methanol, smoke

Citation: Bertschi, I., R. J. Yokelson, D. E. Ward, R. E. Babbitt, R. A. Susott, J. G. Goode, and W. M. Hao, Trace gas and particle emissions from fires in large diameter and belowground biomass fuels, *J. Geophys. Res.*, *108*(D13), 8472, doi:10.1029/2002JD002100, 2003.

1. Introduction

[2] The Earth's atmosphere is a complex mixture of gases and particles from many natural and anthropogenic sources. Since the emergence of plant life from the oceans, fires have strongly influenced the atmosphere [*Wallace and Hobbs*, 1977]. The past several decades have seen rapidly expanding research into how biomass fire emissions affect the physics and chemistry of the atmosphere. It is now well known that biomass fires emit globally significant amounts of carbon dioxide (CO_2), carbon monoxide (CO), nitrogen oxides (NO_x), methane (CH_4), nonmethane hydrocarbons (NMHC), oxygenated volatile organic compounds (OVOC), and reduced nitrogen-containing species such as ammonia (NH_3) and hydrogen cyanide (HCN) [*Crutzen and Andreae*, 1990; *Yokelson et al.*, 1996, 1999; *Holzinger et al.*, 1999]. Several of these gases contribute to the greenhouse effect. Additionally, biomass fire emissions influence the amount of tropospheric ozone (O_3), which is a greenhouse gas and a reactive oxidant involved in many photochemical processes [*Stith et al.*, 1981; *Delany et al.*, 1985; *Finlayson-Pitts and Pitts*, 1986; *Fishman et al.*, 1991; *Mason et al.*, 2001]. Biomass burning also produces large amounts of particles that influence the radiative properties of the atmosphere and,

[1]Department of Chemistry, University of Montana, Missoula, Montana, USA.
[2]Now at Interdisciplinary Arts and Sciences, University of Washington-Bothell, Bothell, Washington, USA.
[3]Fire Sciences Laboratory, U.S. Department of Agriculture (USDA) Forest Service, Missoula, Montana, USA.
[4]Now at Enviropyronics, LLC, White Salmon, Washington, USA.
[5]Now at Bruker Optics, Inc., Billerica, Massachusetts, USA.

0148-0227/03/2002JD002100

thus, the global climate [*Kaufman and Nakajima*, 1993; *Charlson et al.*, 1992].

[3] Nearly all previous field and laboratory studies of biomass burning quantified the emissions and/or fuel consumption for fires burning mostly in surface and aboveground, fine fuels (i.e., grasses, litter, shrubs, and foliage). In these fires, more than 80% of the fuels are normally consumed by flaming combustion and most of the emissions are entrained in a convection column associated with large flaming fronts. This study focuses on a different type of biomass combustion. Specifically, stumps, logs, downed branches, and "belowground biomass" (duff, roots, and organic soils) can smolder long after flaming and strong convection from a burned area has ceased. The phenomenon of smoldering combustion that consumes biomass (and produces smoke) at any location that is no longer influenced by the strong convection associated with a flame front has been defined as residual smoldering combustion (RSC) [*Wade and Lunsford*, 1989]. RSC has also been defined as "independent smoldering combustion not requiring a flame" [*Sandberg*, 1983]. We adopt the former definition of RSC for this atmospheric study because it is more closely related to the weak convection that normally characterizes the dispersion of the smoke that is produced. RSC can occur when a fire is producing a convection column that is unable to draw in all the fire emissions or after all strong convection from the fire has ceased.

[4] Several studies have already shown that RSC can be responsible for much of the fuel consumption in fires that have considerable atmospheric significance. For instance, *Kauffman et al.* [1998] reported that pasture maintenance burns on the site of former tropical woodlands are the most prevalent use of fire in the Brazilian Amazon and that RSC of large diameter woody fuels accounted for up to 38–44% of the biomass consumed by these fires. Typically, the original forests on these sites are slashed at the beginning of the dry season and burned after 2–3 months of drying [*Kauffman et al.*, 1995]. Large woody fuels remain and they are gradually consumed in pasture maintenance fires in subsequent years. Eventually the site is degraded and abandoned and a new pasture is established. The smoldering combustion of dead woody fuels is a significant part of each fire in the cycle and it often lasts for days or weeks after flaming combustion has subsided [*Ward et al.*, 1992; *Kauffman et al.*, 1994; *Barbosa and Fearnside*, 1996; *Guild et al.*, 1998; *Carvalho et al.*, 1998]. *Levine* [1999] estimated that 89% of the smoke in the extensive 1997 haze event in southeast Asia was produced by peat fires, which would probably involve RSC. Therefore, it seems likely that both global deforestation and pasture maintenance in former woodlands produce large amounts of RSC emissions. RSC has also been reported to consume over 50% of the biomass in temperate and boreal fires [*Sandberg*, 1983; *Fransden*, 1991; *Reinhardt et al.*, 1991; *Kasischke et al.*, 1999] (Sandberg, personal communication, 2001). Many smoke management problems associated with prescribed fires in the United States (e.g., smoke impacting highways or towns) involve RSC [*Hardy et al.*, 2002].

[5] To our knowledge, despite the importance of RSC, comprehensive measurements of RSC emissions were not available when this work began. Several factors contributed to this lack of data. Many previous measurements of biomass burning emissions relied on airborne sampling, which can only sample the emissions lofted by convection. However, RSC emissions (according to our definition) are not influenced by strong, fire-induced convection and, at least initially, stay near the ground. Quantifying site average RSC emissions in a ground-based field experiment would have required characterizing many point sources distributed over a large, remote area for many days with variable winds. As a result of the lack of data, atmospheric chemistry and smoke production models were (implicitly or explicitly) based on very uncertain assumptions about RSC emissions.

[6] Because of the general need to better understand biomass burning, and also increased public concern about the impacts of smoke on air quality, we recently carried out laboratory and field studies dedicated explicitly to RSC. We report preliminary observations regarding a few key environmental variables that influence the extent of RSC in fires and the first comprehensive measurements of the emissions from the RSC of RSC-prone fuels. Specifically, we used filter sampling and spectroscopic techniques to measure PM2.5 (particles with diameter < 2.5 μm), CO_2, CO, CH_4, NMHC, OVOC, NH_3, and HCN emitted by RSC of large diameter logs, wood debris, duff, and organic soils in a controlled laboratory setting where we could capture and analyze all the emitted smoke. We also report field measurements of RSC at an African woodland site made during September 2000 as part of SAFARI 2000. Our RSC emission factors (EF) for many species are quite different than the EF measured during the "non-RSC" portion of similar fires. The large impact this can have on biomass burning emissions estimates is demonstrated with a few examples.

2. Experimental

2.1. Fuel Characteristics

[7] We selected fuels for the laboratory fires that represent the types of biomass most commonly consumed by RSC (Table 1). We burned three duff samples from a pine/fir forest in Montana and two organic soil samples from a jack pine forest floor near Fort Providence, Northwest Territories, Canada. We burned a stump (35 cm diameter, 40 cm height) along with the surrounding duff that was extracted from a Montana pine forest. Our other wood fuels were large diameter, dead hardwood logs collected from a riparian zone outside Missoula, MT and smaller diameter softwood debris (partially decayed) sampled from a pine/larch forest in rural western Montana. We measured the moisture, carbon, hydrogen, and nitrogen content of many of the fuels with the exception of the miombo logs.

[8] In addition to our fire-integrated laboratory measurements, we made spot measurements of the RSC emissions, in situ, from a group of smoldering large diameter (>30 cm) logs in a wooded savanna (miombo) in Zambia, Africa approximately 3 days after a flaming front had passed through the area igniting the logs. Similar dead and downed logs likely account for nearly all the RSC that occurs in Zambia's tropical woodlands.

2.2. Laboratory Sampling Platforms

[9] As noted above, most of the fires were burned at the USDA Forest Service Fire Science Laboratory (FSL). The

Table 1. Fuels Prone to RSC That Were Burned in This Study[a]

Fire Name	Fuel Type	Sample Location	Overstory/Understory	Fuel Properties			Combustion Factor (%)[b]
				%C	%N	$\%H_2O$	
Lolo 1	Duff/Organic Soil	Lolo National Forest, Lolo Pass, Montana	Lodgepole Pine/Subalpine fir (*Pinus contorta*/*Abies lasiocarpa*)	47.6[c]	1.22[d]	8.5	45.8
Lolo 2				48.3[c]	1.22[d]	8.2	47.5
Lolo 3				48.8[c]	1.22[d]	11.4	65.4
NWT 1	Duff/Organic Soil	Fort Providence, Northwest Territories, Canada	Jack Pine/Black Spruce (*Pinus banksiana*/*Picea mariana*)	45.3[c]	1.67[d]	18.8	76.4
NWT 2				48.8[c]	1.67[d]	9.1	10.2
Stump	Mixture of Softwood/ Duff/Organic Soil	Blue Mountain, Missoula, MT	Douglas fir/Pinegrass (*Pseudotsuga menziesii*/ *Calamagrotis rubesceus*)	50[e]		70.6[f] 25.3[g]	79.8
Cottonwood Log 2	Large Diameter (>30 cm) Hardwood Logs	USDA FSL, Missoula, Montana	Black Cottonwood (*Populus balsamifera*)	50[e]	0.04[d]		94.2
Zambia Log	Large Diameter (>30 cm) Hardwood Logs	Wooded Savanna, West Central Zambia, Africa	*Julbernardia globiflora*, *Brachystegia* sp.	50[e]			
PC 1	Softwood Debris	Plum Creek, Inc. Timberland, Seeley Lake, MT	Larch, Ponderosa Pine, Douglas fir (*Larix occidentalis*, *Pinus* sp., *Pseudotsuga menziesii*)	50[e]			90.6
PC 2				50[e]			94.2

[a]Blank indicates not measured.
[b]The combustion factor is defined here as the percentage of the fuel actually exposed to fire that was volatilized. For the duff, organic soils, and stump fire, the fuel includes all the material above the mineral soil and there was a large residual mass that included ash and char.
[c]Based on analysis of the sample that was burned.
[d]Based on analysis of a sample similar to the sample that was burned.
[e]Based on the study of *Susott et al.* [1996].
[f]Fuel moisture of wood fuel (stump).
[g]Fuel moisture of duff/organic soil.

FSL combustion facility has a floor area of 12.3 × 12.3 m and a ceiling height of 18.0 m. Outside air is drawn into the room and then exhausted through a stack attached to the ceiling. The stack has an inner diameter of approximately 1.6 m with an ''inverted funnel'' base opening to 3.6 m. The base of the stack was positioned 3 m above a continuously weighed fuel bed situated slightly above floor level. A sampling platform surrounds the stack 15.5 m above the floor where several ports can be used to sample pressure, temperature, and particle and trace gas emissions.

[10] The FSL combustion facility is ideal for measuring the prolonged emissions from RSC of biomass since all of the emissions are entrained into the combustion chamber stack where they become well mixed [*Goode et al.*, 1999] and their composition can be measured for the duration of the fire. However, especially near the end of these very slow burning fires (e.g., consumption rates as low as a few grams per hour), the entrained emissions are so dilute that many species could only be measured with low signal to noise from the sampling platform. Therefore, we employed the following sampling strategy. For each laboratory fire, real-time instruments for CO_2 and CO were deployed on the sampling platform to continuously measure the carbon production profile. The open-path Fourier transform infrared (OP-FTIR) spectrometer was deployed with its optical path spanning the smoke column about one meter above the fires for frequent spot measurements of CO_2, CO and most other stable and reactive gases present above several ppbv. This arrangement optimized the FTIR signal to noise and allowed us to scale the FTIR measurements to the total emissions produced over time.

[11] Our OP-FTIR system consists of an FTIR spectrometer and an open, adjustable path White cell comounted on Super-Invar, Teflon-coated girders. The system was described in detail by *Yokelson et al.* [1997] and only a brief description is given here. The FTIR spectrometer (MIDAC 2500) was used with a spectral resolution of 0.5 cm^{-1} and the open-path White cell had a path length of 51 m for all the laboratory measurements reported here. The entire OP-FTIR system was supported at each end by two mobile carts allowing spectra to be collected alternately for the smoke and chamber ''background'' air. Separate spectra could have been collected every 1.7 s, but that would have generated an enormous volume of data over the period of the RSC fires. Instead, we averaged 100–500 spectral scans for each, alternating, spot measurement of the smoke or background. We acquired many averaged spectra of the emissions during the entire period of RSC of each fire to provide temporal profiles of the trace gases produced. A handheld, chromel-alumel thermocouple positioned close to the White cell path measured the path temperature and pressure was measured with a pressure transducer (Baratron, MKS).

[12] The total CO_2 and CO emitted from the fires was captured, mixed, and exhausted up the stack where it was measured throughout the course of each fire. We measured the carbon production profile with nondispersive infrared (NDIR) CO_2 and CO analyzers (LI-COR, Inc., model 6262; Thermo Environmental Instruments, Inc., model 48C, respectively). A second NDIR CO_2 analyzer was used to measure CO_2 fluctuations in the ambient background air. The temperature, pressure, and the stack flow were measured at the sampling platform using calibrated chromel-alumel thermocouples, pressure transducers (Baratron, MKS), and two mass flowmeters (Kurz, model 455), respectively. A digital scale (Mettler, PM 35) measured the mass loss during the fires. All of these data were logged every 2 s. Teflon filters of the smoke and background air were collected for 10–30 min each at the sampling platform using a cyclone that rejected particles with an effective aerodynamic diameter >2.5 μm at the flow controller set point of 30 L min^{-1}. The flow reading was logged every second so that clogged filters could be identified and rejected. Both the exposed filters and unexposed control filters were weighed before and after the fire in a dedicated room maintained at 50 ± 2% RH and 20°C. Our instrumen-

tation and method for quantifying PM2.5 has been compared to the Federal Reference Method for PM2.5 and has good accuracy [*Trent et al.*, 2000].

2.3. Field Measurements of RSC Emissions in Zambia

[13] We used the OP-FTIR system described above with minor modifications to measure RSC emissions from smoldering logs in a miombo woodland in rural Zambia. Two automotive batteries powered the laptop computer controlling the FTIR data acquisition and the MIDAC spectrometer. We used two shipping crates ($\sim$1 $\times$ 0.5 $\times$ 0.5 m) to elevate the instrument above the smoldering wood debris and optimize the concentration of smoke passing through the FTIR path. Background spectra were collected by deploying the OP-FTIR in a smoke-free area upwind of the emission source. We used a chromel-alumel thermocouple and a portable, digital barometer (Cole-Parmer) to measure temperature and pressure in the FTIR optical path. Individual IR spectra were collected every 0.8 s and subsequently signal averaged as appropriate to improve the signal-to-noise and accuracy of the spectral analysis.

2.4. Retrieval of Excess Mixing Ratios From Spectra

[14] We acquired hundreds of spot measurements of smoke and background air by FTIR (each averaged over 3–15 min) during our laboratory and field measurements of RSC emissions. Mixing ratios for CO_2, CO, and CH_4 were obtained by fitting regions of the transmission spectra with synthetic calibration, classical least squares (CLS) methods described in detail elsewhere [*Griffith*, 1996; *Yokelson et al.*, 1996, 1997; *Yokelson and Bertschi*, 2002]. We take the excess mixing ratios in smoke, for these compounds, to be the smoke mixing ratio minus the background mixing ratio. We also generated absorbance spectra of the smoke (using background spectra obtained between the smoke spectra) and analyzed them by synthetic calibration CLS for formaldehyde (CH_2O), ethane (C_2H_6), acetylene (C_2H_2), hydrogen cyanide (HCN), and ammonia (NH_3) to directly yield excess mixing ratios. In addition, the absorbance spectra were analyzed by spectral subtraction [*Yokelson et al.*, 1997] to directly yield excess mixing ratios for water (H_2O), ethene (C_2H_4), propene (C_3H_6), acetic acid ($CH_3C(O)OH$), methanol (CH_3OH), formic acid (HC(O)OH), phenol (C_6H_5OH), furan (C_4H_4O), glycolaldehyde ($HOCH_2C(O)H$), and ammonia (NH_3). This suite of compounds accounts for all of the significant features found in our IR smoke spectra, with the exception of a large peak at 2848 cm^{-1} that is yet to be identified. The detection limit for each species varied depending on the amount of signal averaging, fluctuations in the spectrometer performance, and the analysis method. For most compounds the detection limit was in the range 5–20 ppbv and the uncertainty is approximately $\pm$5% (1σ) or the detection limit, whichever is greater.

3. Results and Discussion

[15] We used the excess mixing ratios from each smoke spectrum (or spot measurement) obtained during the fires to calculate spot measurement specific values for emission ratios (ER) between coemitted trace gases; modified combustion efficiency (MCE defined as $\Delta CO_2/(\Delta CO_2 + \Delta CO)$ where Δ indicates an excess value in smoke above background), and EF (g compound per kg fuel (dry weight)). The EF were calculated using the carbon mass balance method [*Ward and Radke*, 1993], which assumes that all the "burned" carbon is volatilized and detected and that the fuel carbon percentage (by mass) is the measured value (Table 1) or 50%. We refer to these spot measurement specific values as "instantaneous" values and abbreviate them as IER, IMCE, and instantaneous EF (IEF). The IEF calculated in this manner for CO_2 and CO were in good agreement with IEF calculated from the NDIR and mass loss data. The instantaneous values changed slowly, but significantly over the course of most fires as discussed in section 3.1 (see Figures 1–4).

[16] We also calculate ER, MCE, and EF that are representative of all the fuel consumed by RSC for each entire fire. To do this we used weighted averaging as follows. Each spectrum was assumed valid for the time it was collected and for one half of any unmeasured time interval before and after the spectrum. The sum of the CO_2 and CO production measured by the real time instruments over this time period was assumed to be proportional to fuel consumption during that period and was used as the weighting factor. (For the field measurements of the smoldering miombo logs, we assumed the weighting factors were equal as justified in section 3.1.) The weighted average ER was then used to calculate weighted average MCE and EF. Table 2 lists these RSC average ER, MCE, and EF for each fire. We denote these quantities as ER_{RSC}, MCE_{RSC}, and EF_{RSC}, respectively. We will use the instantaneous values to show important trends in the emissions during a fire and the RSC average values to compare with integrated values from other types of fires and (in combination with estimates of fuel consumption by RSC) to estimate the effect of RSC on total emissions.

[17] Previous work usually reported fire-integrated ER, MCE, and EF, which were representative of entire fires in aboveground fine fuels that did not feature RSC. Under those conditions, the fire-integrated MCE values are useful as an indicator of the relative amount of flaming and smoldering over the course of the fire. Further, *Yokelson et al.* [1996, 1997, 1999] and *Goode et al.* [2000] reported a high correlation between the fire-integrated MCE and the fire-integrated EF for various compounds. In contrast, in this work, the RSC average quantities should represent the entire RSC process and the MCE are simply typical values for "pure" smoldering combustion.

3.1. Chemistry and Physics of RSC

3.1.1. Initiation and Duration of RSC

[18] In nature, RSC is usually initiated by flaming combustion of fine, surface fuels. To mimic this, we started each lab RSC fire by igniting 200 g of dry fine fuels on top of the RSC-prone fuel. (Emissions measurements began after the starter fuel was consumed and combustion of the RSC-prone fuel had commenced.) We burned additional experimental fires to explore the effects of a few, key physical variables. We found that low fuel moisture in organic soils [*Fransden*, 1987, 1997] and decomposition of woody fuels promoted easier ignition of the target fuels. In contrast, postignition fuel consumption was heavily dependent on whether fuel geometry promoted efficient heat transfer. For instance, dry, sound wooden blocks were only slightly

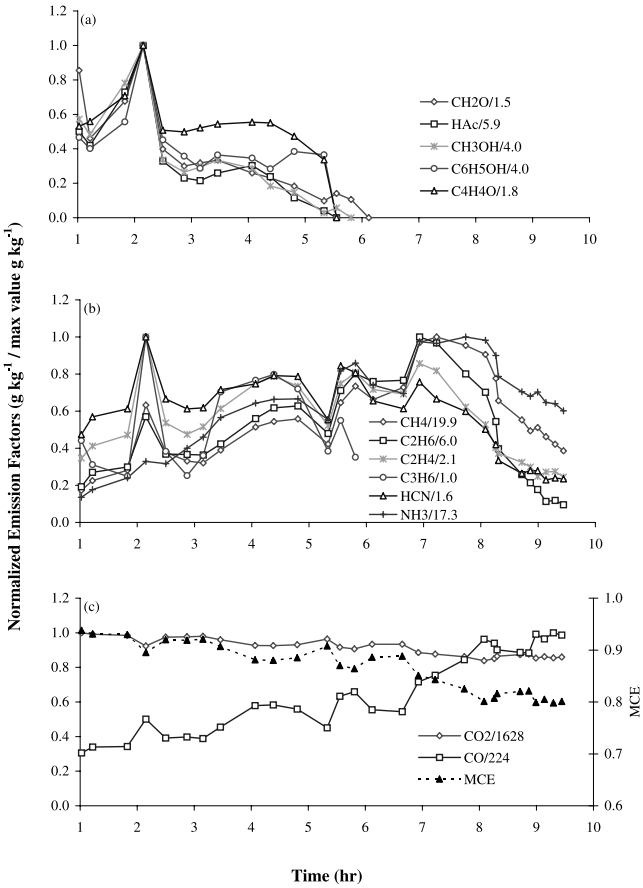

Figure 1. The trace gases detected by OP-FTIR in the smoke from the Northwest Territories Organic Soil 1 fire are shown as normalized IEF versus hours since ignition. (Specifically, each IEF is divided by the maximum IEF, which is shown in the legend.) The emissions are grouped according to their formation process: (a) the products of low-temperature pyrolysis of fresh biomass, which creates "low-temperature char," (b) the products of high-temperature pyrolysis of low-temperature char, and (c) the products of gasification. Part (c) also shows the MCE.

charred when they were placed 7 cm apart directly above small "starter fires." More than 50% of identical blocks were consumed by RSC if they were placed only 1 cm apart directly above identical starter fires. These observations are mentioned because, ultimately, fuel moisture, fuel geometry classifications, and other key environmental variables found to affect RSC might be mapped over large regions by remote sensing. In view of the large effect RSC can have on emissions estimates, such an effort could be warranted.

3.1.2. Combustion Processes and Emissions During RSC

[19] In this section, we describe and interpret the degree of variability in the IEF observed during the lab fires. The combustion of biomass involves many different chemical and physical processes that release many different particles and trace gases. To aid in assigning the emissions to specific processes, we describe the progression of emissions from an individual element of biomass as its temperature is rapidly raised (as would occur during a fire). *Yokelson et al.* [1996, 1997] described this previously and we offer a summary here. Distillation occurs when the biomass temperature is raised enough to exceed the boiling point of bound liquids. For instance, the fuel moisture will begin to "boil off" when the temperature reaches 100°C. At 100–200°C, the biomass begins to undergo pyrolysis, which is the thermal cleavage of molecular bonds in the cellulosic and lignin macromolecules that make up the solid biomass. Low-temperature pyrolysis (primarily occurring at 200–300°C) releases a white smoke, which is a complex, flammable mixture including reflective aerosol, low molecular weight oxygenated organic compounds, and water. The composition of these pyrolysis products is influenced by the temperature (or rate of change in temperature) and the chemical composition of the biomass [*Overend et al.*, 1995]. The release of oxygenated compounds and water by low-temperature pyrolysis produces a carbon-enriched, solid intermediate called "low-temperature char" that has high aliphatic content. When temperatures reach 400–600°C, the "low-temperature char" is subjected to "high-temperature pyrolysis," which produces gas-phase products such as alkanes and a solid intermediate called "high-temperature char" that is high in aromatic content. Once char is formed, "gasification" can begin to accompany pyrolysis. This is because the exothermic chemisorption of O_2 on char provides energy for gasification reactions in which solid char is converted to gas-phase products such as H_2, CO_2, CO, and H_2O. "Glowing combustion" is simply a popular term

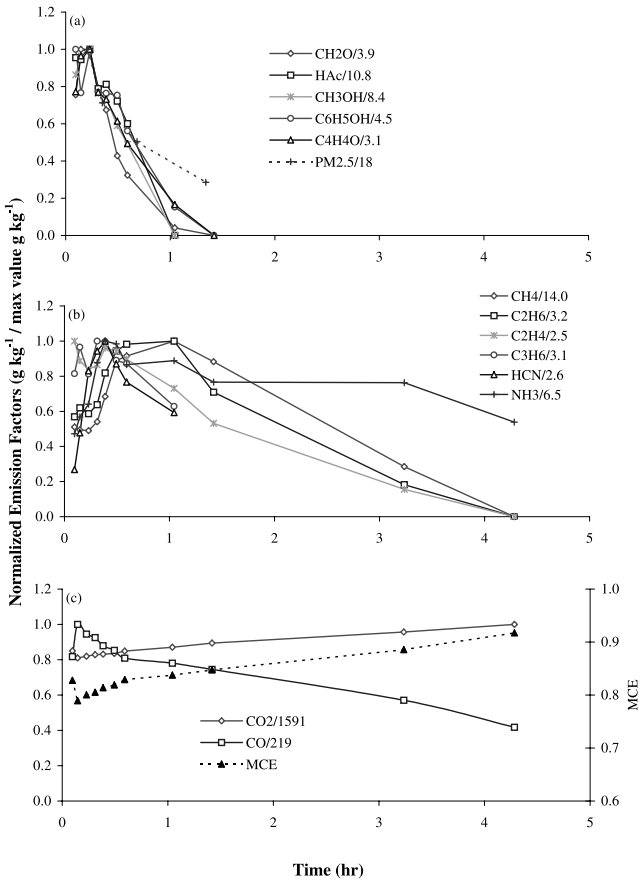

Figure 2. As in Figure 1, but for the Lolo Duff 1 fire.

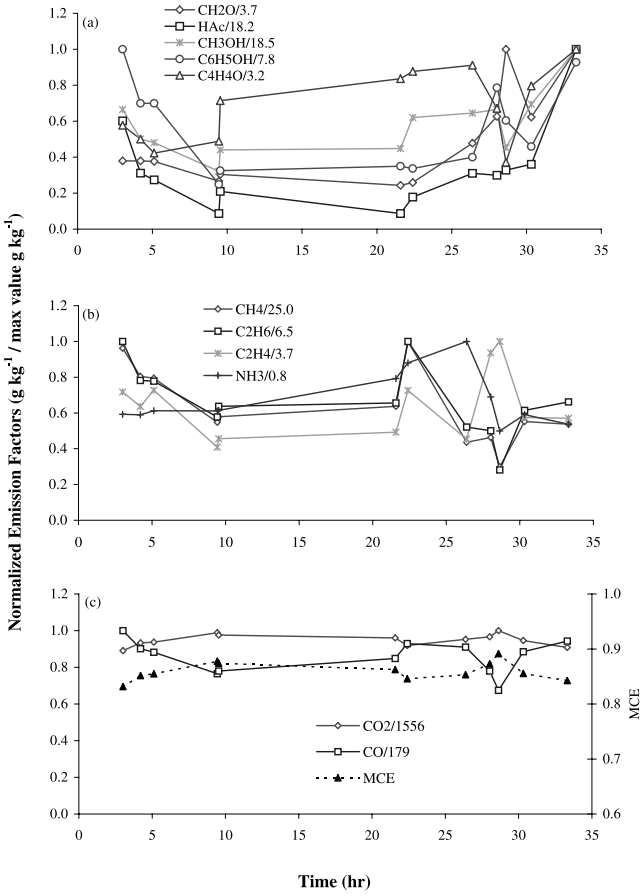

Figure 3. As in Figure 1, but for the Cottonwood Log 2 fire.

indicating gasification of sufficient intensity to emit visible light. The combination of gasification and high-temperature pyrolysis produces a faint bluish white smoke.

[20] In biomass fires, low- and high-temperature pyrolysis and gasification all produce flammable gases from biomass. Often, these gases are entrained in turbulent, diffusion flames and oxidized to CO_2, H_2O, and NO. Under these circumstances, both the flames and gasification supply the heat that drives pyrolysis. The combination of all these processes is commonly called "flaming combustion." In the absence of flames, the products of pyrolysis and gasification directly enter the atmosphere; a situation commonly termed "smoldering combustion." Many of the important differences between biomass fires and industrial combustion are due to significant amounts of smoldering combustion and high oxygen content (~45% dry mass) in biomass. In many of our RSC lab fires, the IEF varied significantly over the course of the fire. Flames were usually absent and we propose that the variation in the IEF could be due to the various smoldering combustion processes coming into dominance at different times.

[21] Figures 1 – 4 illustrate some typical emission profiles for different types of RSC-prone fuels. The data for each of these figures are based on the series of IEF calculated for each species from OP-FTIR spot measurements over the duration of the smoldering fire. Because the IEF may vary by 2 orders of magnitude for the array of compounds measured, the IEF were normalized by plotting each IEF value for a given species i as a fraction of the maximum IEF value for species i measured during a fire (i.e., during measurement interval n, the normalized IEF equals $IEF_{n,i}/IEF_{max,i}$).

[22] Figure 1 shows the IEF versus hours since ignition for the RSC during the first laboratory fire in organic soil from the Northwest Territories. These profiles are typical for RSC of the duff and organic soil samples. After the starter fuel was quickly consumed, a glowing front burned slowly downward from the surface pyrolyzing fresh biomass and generating white smoke ahead of the front. After 6 hours, white smoke production had ceased and the oxygenated compounds were below our detection limits (Figure 1a). We speculate that this coincides with the arrival of the glowing front at the mineral soil. The oxygenates from low-temperature pyrolysis may "disappear" at this point because the fresh biomass may be encapsulated by a char layer and also the emissions are filtered by overlying ash. About 7 hours after ignition the IEF for hydrocarbons begin a steep decline (Figure 1b). This could be because low-temperature char on the surface of the fuel elements is being converted to high-temperature char. Nine hours after ignition, gasification emissions dominate the fire (Figure 1c). This could signal that the surface of all the organic matter has progressed to the high-temperature char stage. Figure 1 shows clearly that an IEF measured at any one point during an organic soil/duff fire could easily be very different from the RSC average EF.

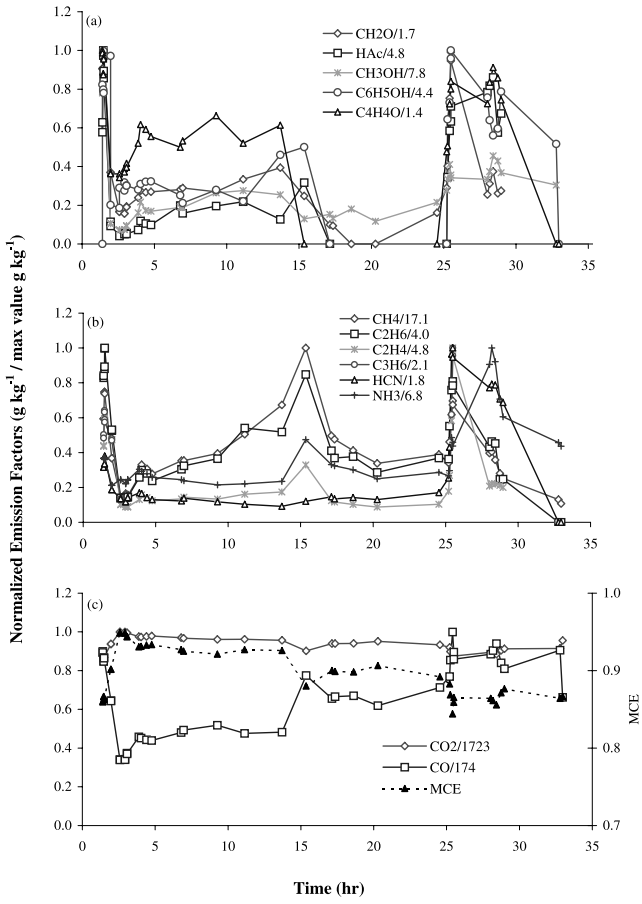

Figure 4. As in Figure 1, but for the Stump fire.

Table 2. Weighted Average ER and EF for RSC of Wood Debris and Duff/Organic Soils[a]

		ER (%)															
		% of CO_2	% of CO														
Fire Name	MCE	CO	CH_4	C_2H_4	C_2H_2	C_3H_6	C_2H_6	CH_2O	GA[b]	HFo[c]	HAc[d]	CH_3OH	C_6H_6O	C_4H_4O	NH_3	HCN
Lolo 1	0.879	13.8	14.1	1.61		1.06	4.60	1.20	0.07	0.08	2.07	2.72	0.57	0.48	6.47	0.96
Lolo 2	0.858	16.5	9.3	1.11		0.45	1.18	0.91	0.07	0.75	1.53	1.98	0.89	0.37	6.74	1.12
Lolo 3	0.857	16.7	4.5	0.63		0.58	0.46	1.09	0.18	0.84	2.29	2.99	0.67	0.40	2.07	1.01
NWT 1	0.891	12.2	14.1	1.01		0.23	2.27	0.41	0.02	0.19	0.60	0.84	0.30	0.24	12.80	0.85
NWT 2	0.848	17.9	6.7	0.80		0.44	1.37	2.58	0.36	1.34	1.95	2.61	0.77	0.36	7.89	1.33
Stump	0.904	10.6	11.9	1.40	0.23	0.33	1.68	0.64	0.02	0.22	0.69	2.18	0.55	0.31	3.30	0.45
Cwd 2	0.854	16.6	18.2	1.52	0.06	1.01	2.66	1.16	0.13	0.46	2.03	6.10	0.92	0.53	0.56	
Zambia Log[e]	0.854	17.1	25.6	1.33		0.86	2.59	2.05		0.44	2.48	4.46	0.42	0.53	1.99	
PC 1	0.861	16.2	2.6	0.19				0.05							0.44	
PC 2	0.861	16.1	6.7	0.21			0.32	0.12	0.06	0.08	0.09	0.37		0.04	0.28	

		EF (g kg^{-1})																
Fire Name	MCE	PM2.5	CO_2	CO	CH_4	C_2H_4	C_2H_2	C_3H_6	C_2H_6	CH_2O	GA[b]	HFo[c]	HAc[d]	CH_3OH	C_6H_6O	C_4H_4O	NH_3	HCN
Lolo 1	0.879	11.3	1454	128	10.4	2.06		2.03	6.32	1.64	0.19	0.17	5.67	3.97	2.44	1.48	5.04	1.19
Lolo 2	0.858	6.6	1460	153	8.2	1.71		1.03	1.94	1.49	0.21	1.89	5.05	3.47	4.59	1.37	6.29	1.66
Lolo 3	0.857		1478	157	4.0	0.99		1.37	0.78	1.84	0.60	2.16	7.72	5.38	3.54	1.53	1.98	1.53
NWT 1	0.891		1436	112	9.0	1.13		0.39	2.71	0.49	0.05	0.34	1.43	1.07	1.14	0.65	8.69	0.92
NWT 2	0.848	15.1	1448	165	6.3	1.32		1.08	2.43	4.56	1.29	3.63	6.90	4.91	4.29	1.44	7.91	2.12
Stump	0.904	15.8	1612	109	7.4	1.53	0.23	0.53	1.96	0.74	0.06	0.39	1.60	2.70	2.02	0.83	2.18	0.47
Cwd 2	0.856		1469	155	16.2	2.36	0.08	2.36	4.42	1.92	0.43	1.16	6.73	10.80	4.78	2.01	0.53	
Zambia Log[e]	0.854		1454	158	23.2	2.11		2.04	4.39	3.48		1.15	8.43	8.09	2.26	2.04	1.92	
PC 1	0.861		1570	162	2.4	0.30				0.09							0.43	
PC 2	0.861		1558	160	6.2	0.33			0.54	0.20	0.21	0.21	0.30	0.68		0.15	0.27	

[a]Blank indicates value below detection limit or not measured.
[b]Glycolaldehyde (other names include hydroxyacetaldehyde and hydroxyethanal).
[c]Formic acid.
[d]Acetic acid.
[e]Reported values are from equally weighted spot field measurements.

[23] Figure 2 shows that the progression of normalized IEF for the Lolo 1 duff fire is similar to that in the (larger) NWT 1 fire. In addition, during the Lolo 1 fire we collected a nearly continuous series of filters. As seen in Figure 2a, the PM2.5 emissions tracked the oxygenated organics (and the presence of visible white smoke) remarkably well. During RSC, the IEFPM2.5 started at a maximum of 17.5 and dropped to 5.0 g kg^{-1}. The RSC average EFPM2.5 for the Lolo duff samples were 6.6 and 11.3 g kg^{-1} (Table 2). The average of these first EF_{RSC} for PM2.5 from duff ($\sim$9 g kg^{-1}) is <70% of the recommended average EFPM2.5 for fires consuming mostly aboveground biomass in extratropical forests (14 g kg^{-1} [*Ward et al.*, 1993] and 13 g kg^{-1} [*Andreae and Merlet*, 2001]). In addition, complete combustion of the duff samples left large amounts of ash and, on average, only volatilized 53% of the total mass of the duff (Table 1). These observations suggest that a significant overestimate of PM2.5 emissions for RSC of duff could result if one used the mass of the duff available and previously reported EFPM2.5 for aboveground biomass. This should be considered when projecting the air quality impacts of boreal forest fires or prescribed fires that involve RSC of duff.

[24] In contrast to the RSC of duff and organic soils, the RSC of the large cottonwood log produced significant emissions of low-temperature pyrolysis products until the end of the fire (Figure 3a). During this fire, the heat from a slowly advancing, glowing front pyrolyzed adjacent areas of fresh biomass and the log was gradually consumed over $\sim$34 hours with a relatively constant proportion of pyrolysis and glowing combustion. Because of the persistence of pyrolysis, the RSC average EF (EF_{RSC}) for the pyrolysis products are generally higher than those reported for the duff fires (Table 2). The EFPM2.5 was not measured, but is probably higher also based on the tracking of PM2.5 with oxygenates noted above. Because of the fairly stable mixture of combustion processes, most of the IEF measured during RSC of the log were within ±20% of the EF_{RSC}. Our field measurements of the smoldering logs in Zambia lasted $\sim$1 hour and produced average EF that were close to the EF_{RSC} for the cottonwood log (Table 2) and, we estimate, within ±20% of the "real" RSC average EF. Finally, we note that the large diameter woody fuels have lower EF for nitrogen-containing compounds. This is probably due to the lower nitrogen content of the woody fuels ($\sim$ 0.05% N) relative to the soil samples (1.0–1.7% N).

[25] Figure 4 shows the temporal profiles of the emissions from the fire that burned a stump and the surrounding duff. The top of the stump was ignited with a propane torch. During the first hour, the fire included pyrolysis, gasification, and small flames and produced large amounts of white, brown and yellowish smoke. The PM2.5 peaked with an IEF of 109 g kg^{-1} during this period. From 1 to 1.5 hours after ignition, the combustion intensity decreased, flaming ceased, and the active front began to include the duff. During this transition, the MCE increased and the IEF for PM2.5 and smoldering products dropped significantly. For the next 14 hours, the emissions followed a modified duff-like profile with an increase in high-temperature pyrolysis products, but the decrease in oxygenates was slowed by the availability of fresh wood in the stump. Twenty hours after ignition, most of the stump had been consumed. The only

visible sign of combustion was faint, bluish white smoke from a depression in the soil where the stump had been. Twenty-five hours after ignition, the combustion rate suddenly increased with small flames and intense pyrolysis and gasification consuming a freshly exposed section of the roots. This was accompanied by a "spike" in the IEF for smoldering products. The rest of the fire involved slow consumption of the remaining duff. The EF_{RSC} values for smoldering compounds from the "stump/duff" fire are closer to the duff fire values than the log values, suggesting that the fire consumed more organic soil than wood.

[26] Finally, we briefly discuss the emissions from the fires in decayed softwood debris (not shown in figures). We collected these samples as part of a project to measure typical fuel moistures for RSC-prone fuels. The decayed softwood debris had relatively high fuel moistures compared to other fuels on the day we sampled. However, these samples were burned several months after having been oven dried for the moisture determination. Consequently, mostly glowing combustion consumed these fuels and these fires had the lowest EF for pyrolysis compounds (Table 2). The results are probably not relevant except for fires in extremely dry field conditions.

3.2. Comparison of RSC Emission Measurements to Other Biomass Burning Emission Measurements

[27] The main goal of this work was to determine if the emissions from RSC (which had not been previously measured) were different from the emissions observed in the many previous studies of biomass burning that did not include RSC. We address this in two steps. First, using selected OVOC we show that the RSC average EF can indeed be quite different from previously reported fire-integrated EF. Next, we explore the impact that including RSC has on estimates of total fire emissions using a general mathematical approach that shows that RSC can have a widespread and large impact on emissions estimates.

3.2.1. RSC Emissions Compared to Previous Emission Production Models

[28] Previous work showed that for fires in a wide variety of aboveground fine fuels from many temperate and boreal ecosystems, the OVOC EF were tightly correlated with MCE [*Yokelson et al.*, 1996, 1997, 1999, 2003; *Goode et al.*, 1999, 2000] and a single linear regression line was useful for predicting the EF from a wide range of fires. This was particularly true for EF versus MCE for methanol, acetic acid, and formaldehyde (the principal OVOC emitted by fires). Since RSC is a significant component of some fires, it is interesting to determine if EF_{RSC} for OVOC fit the previous models. Figure 5 shows the EF and linear fit from the previous laboratory and airborne FTIR measurements of various aboveground fuels not prone to RSC along with the EF_{RSC} from this study. It is apparent that the EF_{RSC} are not tightly correlated with the previous linear fit and are highly fuel dependent. In general, during RSC, the large diameter woody fuels tend to be consumed by a higher proportion of pyrolysis and have higher OVOC EF than the duff and organic soil fuel types. In summary, the agreement between lab and field measurements is good for both aboveground fine fuels and for RSC-prone fuels, but the simple emissions model for "all" aboveground fine fuels does not work for all RSC-prone fuels because they produce more fuel-dependent values.

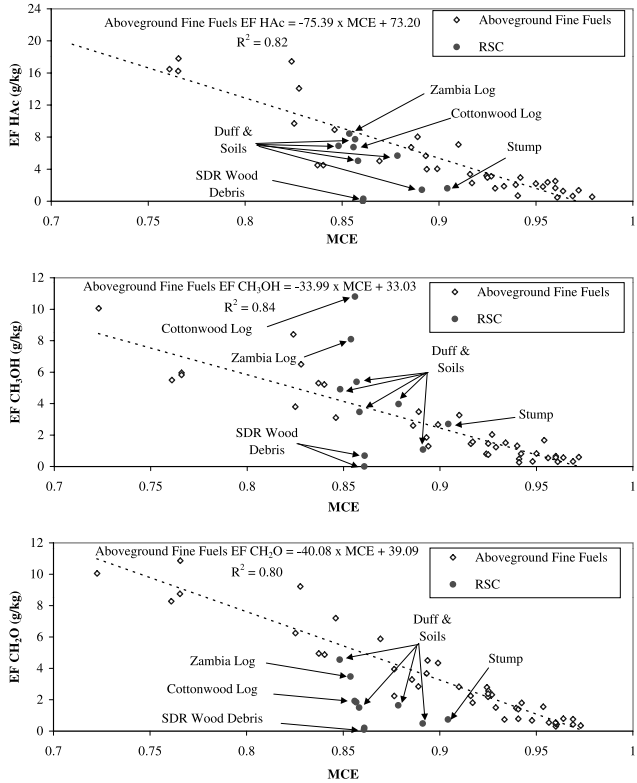

Figure 5. A comparison of the RSC average EF for selected gases to the fire-integrated EF for the same gases measured previously for fires in a wide variety of aboveground fine fuels. The previous data [*Yokelson et al.*, 1996, 1997, 1999; *Goode et al.*, 1999, 2000] are highly correlated with MCE and are fit with a regression line that serves as a simple model for predicting emissions from many different fuel types. The EF for the RSC-prone fuels do not group about the regression line and are highly fuel dependent. ("SDR wood debris" indicates small, dry, and rotted wood debris. These RSC-prone fuels were extremely dry in this study and they burned with a significant amount of flaming and glowing.)

3.2.2. General Significance of RSC Emissions

[29] As noted above, previous studies of the impact of biomass burning on local to global atmospheres relied on available measurements that did not include the emissions from RSC. There were no measurements of the RSC EF and very little data regarding the proportion of biomass consumed by RSC in tropical, boreal, and temperate forest fires. However, if the RSC EF and the proportion of fuel consumed by RSC are known for a fire, then a "true" (or corrected) fire-integrated EF for a given compound i, ($EF_{i,tot}$) can be estimated by coupling this data with data from studies of similar fires that did not include RSC using (1).

$$EF_{i,tot} = (f) \times EF_{i,RSC} + (1 - f) \times EF_{i,conv} \quad (1)$$

$EF_{i,conv}$ and $EF_{i,RSC}$ are the EF measured for compound i in the lofted emissions and during RSC, respectively, and f is

Table 3. Calculated Effect of RSC on Fire-Integrated EF for Boreal Forest and Tropical Wooded Savanna

	CO_2 (g kg^{-1})	CO (g kg^{-1})	NO_x (g kg^{-1})	CH_4 (g kg^{-1})	C_2H_6 (g kg^{-1})	C_2H_4 (g kg^{-1})	C_2H_2 (g kg^{-1})	C_3H_6 (g kg^{-1})	CH_2O (g kg^{-1})	HC(O)OH (g kg^{-1})	$CH_3C(O)OH$ (g kg^{-1})	CH_3OH (g kg^{-1})	NH_3 (g kg^{-1})	HCN (g kg^{-1})
							Boreal Forest[a]							
EF_{conv}[b]	1660	89	1.5	2.8	0.66	1.80	0.24	0.51	1.85	0.99	3.61	1.66	0.86	0.69
EF_{RSC}[c]	1436	112	0.00	9.0	2.71	1.13	0.00	0.39	0.49	0.34	1.43	1.07	8.69	0.92
EF_{tot}	1548	100	0.8	5.9	1.69	1.47	0.12	0.45	1.17	0.67	2.52	1.37	4.78	0.81
EF_{tot}/EF_{conv}	0.93	1.13	0.50	2.11	2.55	0.81	0.50	0.88	0.63	0.67	0.70	0.82	5.55	1.17
							African Miombo[d]							
EF_{conv}[e]	1711	69	3.5	1.4		0.82	0.24		0.75	0.57	2.18	1.03	0.40	0.37
EF_{RSC}[f]	1454	158	0.0	23.2	4.39	2.11	0.00	2.04	3.48	1.15	8.43	8.09	1.92	0.00
EF_{tot}	1685	78	3.2	3.6	0.44	0.95	0.22	0.20	1.02	0.63	2.81	1.74	0.55	0.33
EF_{tot}/EF_{conv}	0.98	1.13	0.90	2.52		1.16	0.90		1.36	1.10	1.29	1.69	1.38	0.90

[a]Assuming RSC of organic soils represents 50% of the total fuel consumption.
[b]The EF for boreal forest fires reported in airborne study of *Goode et al.* [2000].
[c]EF for RSC of boreal forest organic soils from this work.
[d]Assuming RSC of logs represents 10% of the total fuel consumption.
[e]Airborne FTIR measurements of miombo fire EF from the study of *Yokelson et al.* [2003].
[f]EF for smoldering miombo logs from this work.

the fraction of the fuel consumed by RSC. Table 3 illustrates the significance RSC emissions can have by implementing (1) for two "realistic biomass burning scenarios": a boreal forest and an African tropical woodland (miombo).

[30] To develop a realistic estimate of the fraction of total fuel consumption due to RSC for a reasonably common example of a boreal forest fire we note that *Dyrness and Norum* [1983] reported that duff in boreal regions could sustain a spreading fire featuring glowing combustion for many days. In addition, it was recently estimated that 84% of fuel consumption was by RSC during an Alaskan forest fire (Sandberg, personal communication, 2001). Therefore, we make the prognostic assumption that RSC of duff can consume 50% of the fuel in some boreal forest fires. To estimate EF_{RSC}, we use our laboratory measurements for the Northwest Territories 1 fire since it was the boreal forest duff sample that burned in the most representative fashion. (We exclude the NWT 2 fire because an anomalously low percentage of the sample was consumed and without much glowing combustion.) To estimate EF_{conv} we use the Alaskan boreal forest fire, airborne FTIR measurements of *Goode et al.* [2000]. RSC was not thought to be extensive for the early season fires probed by Goode et al., but in any case, they could not probe RSC emissions directly. (The possibility exists that RSC emissions accumulated overnight and were lofted by convective activity the next day). Next, we use (1) to calculate the EF_{tot} (see Table 3). Comparison of EF_{tot} to EF_{conv} suggests that, for a fire of this type, the real fire-integrated emissions of NO_x and OVOC are about one half of what is suggested by airborne sampling alone. On the other hand, the "true" EF for CO, CH_4, C_2H_6, and NH_3 are raised by factors of 1.1, 2.1, 2.6, and 5.6, respectively. *Nance et al.* [1993] reported an airborne measurement of EFPM2.5 of 21 ± 4.8 g kg^{-1} for an Alaskan fire. Since this is higher than any EFPM2.5 obtained in this study, consideration of RSC would probably lower EFPM2.5 for boreal forest fires.

[31] For the wooded savanna example, we use airborne FTIR measurements of miombo fire emissions collected by *Yokelson et al.* [2003] in Zambia during September 2000 for EF_{conv} and our ground-based OP-FTIR spot measurements of smoldering miombo logs for EF_{RSC}. Detailed, fuel consumption measurements made in conjunction with the airborne measurements of *Yokelson et al.* [2003] suggested that perhaps 10% of the fuel consumption on that fire occurred after convection from the site ceased (J. M. C. Pereira et al., Biomass burning parameters of four experimental fires in the Western Province, Zambia, submitted to *International Journal of Wildland Fire*, 2002). Therefore, we implement (1) assuming that RSC of logs represents 10% of the fuel consumed in a miombo fire (see Table 3). The comparison of EF_{tot} to EF_{conv} shows no large decreases in EF. However, there are significant increases for a number of compounds, with CH_4, CH_3OH, and NH_3 increasing by factors of 2.5, 1.7, and 1.4, respectively.

[32] In a previous study, *Hoffa et al.* [1999] reported that grass fire MCE tended to be lower early in the dry season, which could mean that smoldering compounds have higher EF. If lower fuel moistures promote RSC of larger fuels then this could cause higher EF for smoldering compounds later in the dry season.

[33] In summary, "correcting" emissions estimates by including RSC caused large effects in both scenarios; even when RSC consumed only 10% of the fuel. Thus, more measurements of fuel consumption and EF for RSC are needed to improve local to global estimates of biomass fire emissions. In addition, there will be atmospheric effects because the RSC portion of the total fire emissions has different dispersion (e.g., release closer to ground, possible canopy processing, and relatively more release at night).

3.3. Additional Details on the Emissions of Selected Trace Gases

3.3.1. Verification of Significant Phenol Emissions From RSC

[34] In a previous study, *Yokelson et al.* [1997] reported spot measurements of smoldering combustion in many different fuels using OP-FTIR. They observed high concentrations of phenol (C_6H_5OH) emitted from smoldering grass and hardwood fuels and a "study average" ER to CO of 0.69%. This ratio was an order of magnitude higher than the phenol ER reported by *McKenzie et al.* [1995]. In this study, we observe phenol ER to CO (0.3–0.9) (Table 2) from most RSC-prone fuels that are in good agreement with the study average of *Yokelson et al.* [1997]. This confirms that phenol is frequently an important fire emission although it is

emitted at variable levels. *Mason et al.* [2001] used a detailed atmospheric chemistry model to investigate smoke plume photochemistry. They reported that phenol reacts with NO_x within a few hours after emission to form significant amounts of nitrophenol compounds. The fate of the nitrophenols is unknown, but they will probably not rerelease NO_x and, thus, reduce the production of ozone in aged smoke.

3.3.2. FTIR Measurements of Furan in Smoke

[35] Furan (C_4H_4O), an oxygenated heterocyclic organic compound, also appears to be a ubiquitous, but variable, emission from the combustion of RSC-prone fuels. Furan has not been previously detected spectroscopically in biomass burning emissions, but *Greenberg et al.* [1984] reported significant concentrations of furan in field measurements of tropical woodland and grassland fire emissions using electropolished stainless steel canisters for collecting smoke with subsequent trace gas analysis using gas chromatography/flame ionization detection (GC/FID). Our spot measurements of furan ER relative to CO range from 0% to 1.5% and the RSC weighted average values in Table 2 range from 0.24% to 0.53%. These values are close to the average furan ER to CO (0.49%) reported by *Greenberg et al.* [1984] for fires in Brazilian woodlands. *Shepson et al.* [1984] reported that a major source of furan found in forest fire smoke is from the OH-initiated photooxidation of toluene and *ortho*-xylene. However, our measurements in smoke less than 1 s old indicate that a significant amount of furan is produced by low-temperature pyrolysis of biomass (see Figures 1–4).

[36] Furan is a reactive molecule under tropospheric daytime conditions. The major sink of furan is reaction with OH radicals ($k \sim 4 \times 10^{-11}$ cm^3 mol^{-1} s^{-1}) [*Atkinson et al.*, 1983; *Wine and Thompson*, 1984; *Bierbach et al.*, 1992]. This gives an atmospheric lifetime for furan of approximately 7 hours if a 12 hour average OH radical concentration of 1.0×10^6 mol cm^{-3} is assumed. The actual lifetime may be much shorter since OH concentrations are reportedly elevated in fresh smoke plumes [*Mason et al.*, 2001; *Hobbs et al.*, 2003]. *Bierbach et al.* [1995] found that the major products from the OH-initiated photooxidized furan reaction are *cis*- and *trans*-butenedial and maleic anhydride. Since OVOC have a large effect on modeled smoke plume photochemistry [*Mason et al.*, 2001], we will include our furan measurements in future simulations to explore the role furan plays in the chemistry of aged smoke plumes.

3.3.3. Emissions of Nitrogenous Gases From RSC

[37] The major nitrogen-containing gases emitted from biomass burning are N_2, NO_x, and NH_3, and they account for most of the fuel nitrogen volatilized [*Goode et al.*, 1999]. Ammonia and hydrogen cyanide (HCN) were the only nitrogenous species we detected from our fires in RSC-prone fuels. On a molar basis, NH_3 emissions were 5–10 times higher than HCN emissions for our duff and organic soil fires and NH_3 was the only nitrogen-containing species we detected from the smoldering combustion of the woody fuels. These findings confirm previous reports that NH_3 is the major nitrogenous gas produced from smoldering combustion [*Yokelson et al.*, 1996, 1997; *Goode et al.*, 1999, 2000]. Overall, the NH_3 temporal profiles most closely resembled CH_4 profiles during RSC (Figures 1–4), suggesting that NH_3 may be a high-temperature pyrolysis product. We also note that our boreal, organic soil fires emitted significantly more NH_3 than our temperate forest, duff fires; most likely due to the higher nitrogen content in the boreal soils (Tables 1 and 2). Finally, boreal forest fires exert a major influence on the summertime photochemistry of much of the Northern Hemisphere [*Wotawa and Trainer*, 2000; *McKeen et al.*, 2002; *Forster et al.*, 2001] and we suggest that future studies of the regional impact of boreal fires should consider the effect that RSC has on emissions estimates for these fires. This is particularly true for nitrogenous compounds since we estimated that RSC decreased EFNO by a factor of 2 and increased $EFNH_3$ by a factor of ~6 (see section 3.2.2 and Table 3).

4. Conclusions

[38] We adopt a qualitative, working definition of RSC as biomass combustion that produces smoke emissions that are not strongly lofted by fire-induced convection. RSC-prone biomass fuels include duff, organic soils, logs, stumps, and dead woody debris. We cite several previous studies that suggest that RSC probably accounts for a globally important amount of biomass burning.

[39] We used NDIR, filter sampling, and OP-FTIR to make the first measurements explicitly of the trace gas and particle emissions from residual smoldering of the major RSC-prone fuels in our laboratory and in a wooded savanna in Zambia. An important finding was that the distribution of emissions from RSC can sometimes change dramatically over the course of a fire. Taking this into account, we calculated RSC average EF (EF_{RSC}) for the main RSC-prone fuels for PM2.5 and the most abundant trace gas emissions (as determined by FTIR): carbon dioxide, carbon monoxide, methane, ethane, ethene, acetylene, propene, formaldehyde, methanol, acetic acid, formic acid, glycolaldehyde, phenol, furan, ammonia, and hydrogen cyanide.

[40] A significant feature of these results is that the emissions from RSC can be markedly different from previously reported fire EF, which were mainly for fires in aboveground fine fuels. Specifically, the EF_{RSC} for PM2.5 and some trace gases were sometimes much larger or smaller than the EF measured in convection columns above fires in environments similar to those where the RSC-prone fuels were collected. This has important implications for emissions estimates. For example, our newly measured EFPM2.5 for smoldering duff and organic soils is lower than EFPM2.5 for most aboveground biomass fuels. (In addition, the combustion factor (the percentage of fuel exposed to fire that was volatilized) was also lower for duff and organic soils (50–75% by mass) than for aboveground fine fuels.) These observations suggest that using previously measured EFPM2.5 coupled with the mass of the available duff would significantly overestimate the PM2.5 emissions from these types of fires.

[41] Finally, we demonstrate a general method for refining emissions estimates using our EF_{RSC} and estimates of fuel consumption by RSC. Application of this method in two examples shows that consideration of RSC can have a large impact on estimates of biomass burning emissions. For instance, assuming that RSC accounts for 50% of fuel

consumption in a boreal forest fire reduces the NO_x EF by one half and increases $EFNH_3$ by almost a factor of 6. Assuming that only 10% of the fuel is consumed by RSC in an African wooded savanna increases the CH_4 EF by a factor of 2.5. These examples clearly demonstrate that additional measurements of the EF and fuel consumption due to RSC should be stressed in future biomass burning research.

[42] **Acknowledgments.** This research was supported by funds provided by the National Science Foundation under grants ATM-9631219 and ATM-9900494, the Rocky Mountain Research Station, Forest Service, U.S. Department of Agriculture (INT-97082-RJVA and RMRS-99508-RJVA), and the interagency Joint Fire Science Program. The authors thank SAFARI 2000 and Geoff Richards for informative discussions on the chemistry of smoldering combustion, Jim Reardon for the duff and organic soil samples, and Michael Chandler for helping extract the stump/duff sample burned in this work.

References

Andreae, M. O., and P. Merlet, Emission of trace gases and aerosols from biomass burning, *Global Biogeochem. Cycles*, *15*, 955–966, 2001.

Atkinson, R., S. M. Aschmann, and W. P. L. Carter, Kinetics of the reaction of O_3 and OH radicals with furan and thiophene at 298 ± 2 K, *Int. J. Chem. Kinet.*, *15*, 51–61, 1983.

Barbosa, R. I., and P. M. Fearnside, Pasture burning in Amazonia: Dynamics of residual biomass and the storage and release of aboveground carbon, *J. Geophys. Res.*, *101*, 25,847–25,857, 1996.

Bierbach, A., I. Barnes, and K. H. Becker, Rate coefficients for the gas-phase reactions of hydroxyl radicals with furan, 2-methylfuran, 2-ethylfuran and 2, 5-dimethylfuran at 300 ± 2 K, *Atmos. Environ.*, *26A*, 813–817, 1992.

Bierbach, A., I. Barnes, and K. H. Becker, Product and kinetic study of the OH-initiated gas-phase oxidation of furan, 2-methylfuran and furanaldehydes at ≈300 K, *Atmos. Environ.*, *29*, 2651–2660, 1995.

Carvalho, J. A., N. Higuchi, T. M. Araújo, and J. C. Santos, Combustion completeness in a rainforest clearing experiment in Manaus, Brazil, *J. Geophys. Res.*, *103*, 13,195–13,199, 1998.

Charlson, R. J., S. E. Schwartz, J. M. Hales, R. D. Cess, J. A. Coakley Jr., J. E. Hansen, and D. J. Hofmann, Climate forcing by anthropogenic aerosols, *Science*, *255*, 423–430, 1992.

Crutzen, P. J., and M. O. Andreae, Biomass burning in the tropics: Impact on atmospheric chemistry and geochemical cycles, *Science*, *250*, 1669–1678, 1990.

Delany, A. C., P. Haagensen, S. Walters, A. F. Wartburg, and P. J. Crutzen, Photochemically produced ozone in the emission from large-scale tropical vegetation fires, *J. Geophys. Res.*, *91*, 2425–2429, 1985.

Dyrness, C. T., and R. A. Norum, The effects of fires on black spruce forest floors in interior Alaska, *Can. J. For. Res.*, *13*, 879–893, 1983.

Finlayson-Pitts, B. J., and J. N. Pitts Jr., *Atmospheric Chemistry: Fundamentals and Experimental Techniques*, pp. 142–150, John Wiley, New York, 1986.

Fishman, J., K. Fakhruzzaman, B. Cros, and D. Nganga, Identification of widespread pollution in the Southern Hemisphere deduced from satellite analysis, *Science*, *252*, 1693–1696, 1991.

Forster, C., et al., Transport of boreal forest fire emissions from Canada to Europe, *J. Geophys. Res.*, *106*, 22,887–22,906, 2001.

Fransden, W. H., The influence of moisture and mineral soil on the combustion limits of smoldering forest duff, *Can. J. For. Res.*, *17*, 1540–1544, 1987.

Fransden, W. H., Burning rate of smoldering peat, *Northwest. Sci.*, *65*, 166–172, 1991.

Fransden, W. H., Ignition probability of organic soils, *Can. J. For. Res.*, *27*, 1471–1477, 1997.

Goode, J. G., R. J. Yokelson, R. A. Susott, and D. E. Ward, Trace gas emissions from laboratory biomass fires measured by Fourier transform infrared spectroscopy: Fires in grass and surface fuels, *J. Geophys. Res.*, *104*, 21,237–21,245, 1999.

Goode, J. G., R. J. Yokelson, D. E. Ward, R. A. Susott, R. E. Babbitt, M. A. Davies, and W. M. Hao, Measurements of excess O_3, CO_2, CO, CH_4, C_2H_4, C_2H_2, HCN, NO, NH_3, HCOOH, CH_3OOH, HCHO, and CH_3OH, in 1997 Alaskan biomass burning plumes by airborne Fourier transform infrared spectroscopy (AFTIR), *J. Geophys. Res.*, *105*, 22,147–22,166, 2000.

Greenberg, J. P., P. R. Zimmerman, L. Heidt, and W. Pollock, Hydrocarbon and carbon monoxide emissions from biomass burning in Brazil, *J. Geophys. Res.*, *89*, 1350–1354, 1984.

Griffith, D. W. T., Synthetic calibration and quantitative analysis of gas-phase FTIR spectra, *Appl. Spectrosc.*, *50*, 59–70, 1996.

Guild, L. S., J. B. Kauffman, L. J. Ellingson, D. L. Cummings, E. A. Castro, R. E. Babbitt, and D. E. Ward, Dynamics associated with total aboveground biomass, C, nutrient pools, and biomass burning of primary forest and pasture in Rondonia, Brazil during SCAR-B, *J. Geophys. Res.*, *103*, 32,091–32,100, 1998.

Hardy, C. C., R. D. Ottmar, J. L. Peterson, J. C. Core, and P. Seamon, (eds), *Smoke Management Guide for Prescribed and Wildland Fire: 2001 Edition, PMS 420-2*, 226 pp., Natl. Wildfire Coord. Group, Natl. Interagency Fire Cent., Boise, Idaho, 2002.

Hobbs, P. V., P. Sinha, R. J. Yakelson, T. J. Christian, D. R. Blake, S. Gao, T. W. Kirchstetter, T. Novakov, and P. Pilewskie, Evolution of gases and particles from a savanna fire in South Africa, *J. Geophys. Res.*, *108*, doi:10.1029/2002JD002352, in press, 2003.

Hoffa, E. A., D. E. Ward, W. M. Hao, R. A. Susott, and R. H. Wakimoto, Seasonality of carbon emissions from biomass burning in a Zambian savanna, *J. Geophys. Res.*, *104*, 13,841–13,853, 1999.

Holzinger, R., C. Warneke, A. Hansel, A. Jordan, W. Lindinger, D. H. Scharffe, G. Schade, and P. J. Crutzen, Biomass burning as a source of formaldehyde, acetaldehyde, methanol, acetone, acetonitrile, and hydrogen cyanide, *Geophys. Res. Lett.*, *26*, 1161–1164, 1999.

Kasischke, E. S., K. Bergen, R. Fennimore, F. Sotelo, G. Stephens, A. Janetos, and H. H. Shugart, Satellite imagery gives clear picture of Russia's boreal forest fires, *Eos Trans. AGU*, *80*, 141, 1999.

Kaufman, Y. J., and T. Nakajima, Effect of Amazon smoke on cloud microphysics and albedo-analyses from satellite imagery, *J. Appl. Meteorol.*, *32*, 729–744, 1993.

Kauffman, J. B., D. L. Cummings, and D. E. Ward, Relationship of fire, biomass and nutrient dynamics along a vegetation gradient in the Brazilian cerrado, *J. Ecol.*, *82*, 519–531, 1994.

Kauffman, J. B., D. L. Cummings, D. E. Ward, and R. Babbitt, Fire in the Brazilian Amazon: Biomass, nutrient pools, and losses in slashed primary forests, *Oecologia*, *104*, 397–408, 1995.

Kauffman, J. B., D. L. Cummings, and D. E. Ward, Fire in the Brazilian Amazon, 2, Biomass, nutrient pools and losses in cattle pastures, *Oecologia*, *113*, 415–427, 1998.

Levine, J. S., The 1997 fires in Kalimantan and Sumatra, Indonesia: Gaseous and particulate emissions, *Geophys. Res. Lett.*, *26*, 815–818, 1999.

Mason, S. A., R. J. Field, R. J. Yokelson, M. A. Kochivar, M. R. Tinsley, D. E. Ward, and W. M. Hao, Complex effects arising in smoke plume simulations due to inclusion of direct emissions of oxygenated organic species from biomass combustion, *J. Geophys. Res.*, *106*, 12,527–12,539, 2001.

McKeen, S. A., G. Wotawa, D. D. Parrish, J. S. Holloway, M. P. Buhr, G. Hubler, F. C. Fehsenfeld, and J. F. Meagher, Ozone production from Canadian wildfires during June and July of 1995, *J. Geophys. Res.*, *107*(D14), 4192, doi:10.1029/2001JD000607, 2002.

McKenzie, L. M., W. M. Hao, G. N. Richards, and D. E. Ward, Measurement and modeling of air toxins from smoldering combustion of biomass, *Environ. Sci. Technol.*, *29*, 2047–2054, 1995.

Nance, J. D., P. V. Hobbs, L. F. Radke, and D. E. Ward, Airborne measurements of gases and particles from an Alaskan wildfire, *J. Geophys. Res.*, *98*, 14,873–14,882, 1993.

Overend, R. P., T. A. Milne, and L. K. Mudge, *Fundamentals of Thermochemical Biomass Conversion*, Elsevier Sci., New York, 1995.

Reinhardt, E. D., J. K. Brown, W. C. Fischer, and R. T. Graham, Woody fuel and duff consumption by prescribed fire in northern Idaho mixed conifer logging slash, Res. Pap. INT-443, USDA For. Serv., Int. Res. Stn., Ogden, Utah, 1991.

Sandberg, D. V., Research leads to less smoke from prescribed fires, in *Proceedings, 1983 Northwest Fire Council Annual Meeting 1983 November 21–22, Olympia, Wash.*, 27 pp., Western For. and Conserv. Assoc., Portland, Oreg., 1983.

Shepson, P. B., E. O. Edney, and E. W. Corse, Ring fragmentation reactions on the photo-oxidations of toluene and *o*-xylene, *J. Phys. Chem.*, *88*, 4122–4126, 1984.

Stith, J. L., L. F. Radke, and P. V. Hobbs, Particle emissions and the production of ozone and nitrogen oxides from the burning of forest slash, *Atmos. Environ.*, *15*, 73–82, 1981.

Susott, R. A., G. J. Olbu, S. P. Baker, D. E. Ward, J. B. Kauffman, and R. Shea, Carbon, hydrogen, nitrogen, and thermogravimetric analysis of tropical ecosystem biomass, in *Biomass Burning and Global Change*, edited by J. S. Levine, pp. 350–360, MIT Press, Cambridge, Mass., 1996.

Trent, A., M. A. Davies, R. Fisher, H. Thistle, and R. Babbitt, Evaluation of optical instruments for real-time, continuous monitoring of smoke particulates, Tech. Rep. 0025-2860-MTDC, 38 pp., USDA For. Serv., Missoula Technol. and Dev. Cent., Missoula, Mont., 2000.

Wade, D. D., and J. D. Lunsford, A guide for prescribed fire in southern forests, R8-TP-11, USDA For. Serv. Tech. Publ., Washington, D. C., 1989.

Wallace, J. M., and P. V. Hobbs, *Atmospheric Science: An Introductory Survey*, Academic, San Diego, Calif., 1977.

Ward, D. E., and L. F. Radke, Emissions measurements from vegetation fires: A comparative evaluation of methods and results, in *Fire in the Environment: The Ecological, Atmospheric and Climatic Importance of Vegetation Fires*, edited by P. J. Crutzen and J. G. Goldammer, pp. 53–76, John Wiley, New York, 1993.

Ward, D. E., R. A. Susott, J. B. Kauffman, R. E. Babbitt, D. L. Cummings, B. Dias, B. N. Holben, Y. J. Kaufman, R. A. Rasmussen, and A. W. Setzer, Smoke and fire characteristics for cerrado and deforestation burns in Brazil: Base-B experiment, *J. Geophys. Res.*, *97*, 14,601–14,619, 1992.

Ward, D. E., J. Peterson, and W. M. Hao, An inventory of particulate matter and air toxic emissions from prescribed fires in the USA for 1989, in *Proceedings of the Air and Waste Management Association, Denver, Colo.*, June 14–18, Air and Waste Manage. Assoc., Pittsburgh, Pa., 1993.

Wine, P. H., and R. J. Thompson, Kinetics of OH reactions with furan, thiophene, and tetrahydrothiophene, *Int. J. Chem. Kinet.*, *16*, 867–878, 1984.

Wotawa, G., and M. Trainer, The influence of Canadian forest fires on pollutant concentrations in the United States, *Science*, *288*, 324–328, 2000.

Yokelson, R. J., and I. Bertschi, Vibrational spectroscopy in the study of fires, in *Handbook of Vibrational Spectroscopy*, vol. 4, edited by P. Griffiths and J. Chalmers, pp. 2879–2886, John Wiley, New York, 2002.

Yokelson, R. J., D. W. T. Griffith, and D. E. Ward, Open-path Fourier transform infrared studies of large-scale laboratory biomass fires, *J. Geophys Res.*, *101*, 21,067–21,080, 1996.

Yokelson, R. J., R. Susott, D. E. Ward, J. Reardon, and D. W. T. Griffith, Emissions from smoldering combustion of biomass measured by open-path Fourier transform infrared spectroscopy, *J. Geophys. Res.*, *102*, 18,865–18,877, 1997.

Yokelson, R. J., J. G. Goode, D. E. Ward, R. A. Susott, R. E. Babbitt, D. D. Wade, I. Bertschi, D. W. T. Griffith, and W. M. Hao, Emissions of formaldehyde, acetic acid, methanol, and other trace gases from biomass fires in North Carolina measured by airborne Fourier transform infrared spectroscopy, *J. Geophys. Res.*, *104*, 30,109–30,125, 1999.

Yokelson, R. J., I. Bertschi, T. C. Christian, P. V. Hobbs, D. E. Ward, and W. M. Hao, Trace gas measurements in nascent, aged, and cloud-processed smoke from African savanna fires by airborne Fourier transform infrared spectroscopy (AFTIR), *J. Geophys. Res.*, *108*, doi:10.1029/2002JD002322, in press, 2003.

R. E. Babbitt, W. M. Hao, and R. A. Susott, Fire Sciences Laboratory, U.S. Department of Agriculture (USDA) Forest Service, Missoula, MT, USA.

I. Bertschi, Interdisciplinary Arts and Sciences, University of Washington-Bothell, Bothell, WA, USA.

J. G. Goode, Bruker Optics, Inc., Billerica, MA, USA.

D. E. Ward, Enviropyronics, LLC, White Salmon, WA, USA.

R. J. Yokelson, Department of Chemistry, University of Montana, Missoula, MT, USA. (byok@selway.umt.edu)